Suppression of the Hanle Effect in Organic Spintronic Devices

Z. G. Yu

SRI International, 333 Ravenswood Avenue, Menlo Park, California 94025, USA

(Received 28 February 2013; published 2 July 2013)

We study carrier spin transport under a transverse magnetic field in organic structures. In organics, carriers are localized polarons and charge transport is via polaron hopping. Spin transport, however, can utilize the exchange coupling between localized polarons, which can be much faster than polaron hopping and rapidly increases with the carrier density. Consequently, a much stronger magnetic field is needed to modify spin polarization and observe the Hanle effect than estimated from the carrier mobility, which can help with the understanding of recent Hanle measurements in organic spin valves. The exchange-induced spin transport also greatly mitigates the conductivity mismatch between ferromagnets and organics, enabling spin injection into organics.

DOI: 10.1103/PhysRevLett.111.016601 PACS numbers: 72.80.Le, 72.25.Dc, 75.30.Et, 75.40.Gb

Efficient spin injection (SI) is a prerequisite for many spintronic devices [1]. SI from ferromagnets into inorganic semiconductors has been convincingly demonstrated by the Hanle effect (HE), where the device resistance is strongly influenced by the spin precession caused by a transverse magnetic field B [2–5]. In a spin-valve structure, the HE is expected to occur when the time period of spin precession is comparable to the time required for carriers to traverse the device, $\omega \equiv \gamma_e B \sim D_h/L^2$, where γ_e is electron gyromagnetic ratio, D_h is the carrier diffusion constant, and L is the channel length [6]. Organic spintronics has attracted considerable interest because of weak spin-orbit and hyperfine interactions in organics [7]. While a pronounced magnetoresistance (MR) in thick ($L \sim 100$ nm) organic spin valves (OSVs) has been frequently observed [8–13], a disturbing puzzle is that the device resistance is independent of B up to 10 mT [14,15], or $\omega \sim 10^9$ Hz, which is several orders of magnitude larger than D_h/L^2, estimated to be $\sim 10^2$ Hz for a typical carrier mobility $\nu_h \sim 10^{-6}$ cm^2/V s at $T = 100$ K [16]. The absence of HE casts doubt on genuine SI in OSVs. On the other hand, muon spin rotation clearly sees injected spins in the organic [11]. In fact, SI into OSVs itself is puzzling, for the low carrier mobility in organics suggests an enormous conductivity mismatch between ferromagnets and organics, which makes SI virtually impossible [17]. In this Letter, we show that spin transport in OSVs is fundamentally different from that in inorganic SI structures: The exchange coupling between localized carriers in organics can facilitate a rapid spin transport, which significantly suppresses the HE and tremendously alleviates the conductivity mismatch obstacle to SI in OSVs.

The organic material in an OSV is a disordered film, in which carriers (polarons), while mobile, are very localized. This is distinct from inorganic SI structures, where carriers are delocalized Bloch waves. The localized polarons give rise to an exchange coupling when they are close to one another. Consider two polarons with opposite spins on two molecules l and m initially, $|l\uparrow; m\downarrow\rangle$. The exchange coupling can flip the spins and change the state into $|l\downarrow; m\uparrow\rangle$. Effectively, the up (down) spin moves from l (m) to m (l), resulting in a net spin current from l to m. This process does not change the carrier occupations and therefore entails no charge motion. Polaron hopping, however, moves charge and spin *simultaneously*. Hence when the exchange-induced spin motion is more rapid than the polaron hopping, the spin and charge transport in organics may be well *decoupled*. No such decoupling will occur in the inorganic structures.

Spin transport due to exchange and hopping can be more rigorously discussed on an equal footing by using a density matrix in the spin space, $\hat{\rho}_i = f_i^0(\hat{1} + \hat{\boldsymbol{\sigma}}\cdot\boldsymbol{M}_i)/2$, to describe spin-polarized polarons. Here f_i^0 and $\boldsymbol{M}_i$ are the polaron occupation and spin polarization at molecule i. $\boldsymbol{M}_i$ is related to the spin-polarized electrochemical potential $\boldsymbol{\mu}_i$ via $\boldsymbol{M}_i = \boldsymbol{\mu}_i/k_BT$, with k_B being the Boltzmann constant. The Hamiltonian of the organic is $H = H_0 + H_h + H_e$,

$$H_0 = \sum_i [E_i(a_{i\uparrow}^\dagger a_{i\uparrow} + a_{i\downarrow}^\dagger a_{i\downarrow}) + \hbar\hat{\boldsymbol{S}}_i\cdot\boldsymbol{\omega}], \tag{1}$$

$$H_h = \sum_{\langle ij\rangle s} V_{ij}(a_{is}^\dagger a_{js} + a_{js}^\dagger a_{is}), \tag{2}$$

$$H_e = \sum_{lm} J_{lm}\hat{\boldsymbol{S}}_l\cdot\hat{\boldsymbol{S}}_m, \tag{3}$$

where $a_{is}^\dagger$ creates a polaron with spin s on molecule i, E_i is the polaron energy, $\hat{\boldsymbol{S}}_i = \sum_{ss'} a_{is}^\dagger\hat{\boldsymbol{\sigma}}_{ss'}a_{is}/2$ is the spin operator of the polaron with $\hat{\boldsymbol{\sigma}}$ being the Pauli matrices, and $\boldsymbol{\omega}$ is the spin Larmor frequency under the transverse magnetic field $\boldsymbol{B}$. V_{ij} in H_h describes polaron hopping between adjacent molecules i, j. J_{lm} in H_e is the exchange between polaron spins on molecules l and m [18].

By treating $H_{\rm int} \equiv H_h + H_e$ as perturbation, the dynamics of $\hat{\rho}_i$ can be obtained by solving the Redfield equation

in the interaction representation [19], $(d\hat{\rho}_i^*/dt) = -\int_0^\infty d\tau \overline{[H_{\rm int}^*(t), [H_{\rm int}^*(t-\tau), \hat{\rho}_i^*(0)]]}$, where $\hat{O}^*(t) \equiv e^{iH_0 t}\hat{O}e^{-iH_0 t}$ for an operator $\hat{O}$ and the line means ensemble average. A phonon bath is assumed to couple to the system for a definite temperature. The charge dynamics obeys the usual master equation, $(df_i^0/dt) = -\sum_j [f_i^0(1-f_j^0)w_{ij} - f_j^0(1-f_i^0)w_{ji}]$, where w_{ij} is the hopping rate from site i to j and can be expressed as $w_{ij} = \int_{-\infty}^{+\infty} d\tau \overline{V_{ij}(t)V_{ji}(t-\tau)}e^{-i(E_i-E_j)\tau}$ [19]. In the absence of charge current, the occupation follows the Fermi-Dirac distribution $f_i^0 = [1+e^{-(E_i-\mu_0)/k_BT}]^{-1}$ with μ_0 being the Fermi level of the system. The dynamics of spin polarization $\boldsymbol{M}_i$ in this situation satisfies

$$\frac{d\boldsymbol{M}_i}{dt} = \boldsymbol{M}_i \times \boldsymbol{\omega} - \sum_j w_{ij}(1-f_j^0)(\boldsymbol{M}_i - \boldsymbol{M}_j) - \sum_l f_l^0 \eta_{il}(\boldsymbol{M}_i - \boldsymbol{M}_l), \quad (4)$$

where we have used $\overline{\hat{S}_l^p \hat{S}_m^q} = \delta_{lm}\delta_{pq} f_l^0 S(S+1)/3$ ($p, q = x, y, z$ and $S = 1/2$), and

$$\eta_{il} = \int_{-\infty}^{+\infty} d\tau \overline{J_{il}(t)J_{il}(t-\tau)}. \quad (5)$$

Equation (4) indicates that both polaron hopping and exchange contribute to spin transport with the former taking place between occupied and unoccupied adjacent molecules and the latter between occupied molecules. The temporal correlation in Eq. (5) accounts for the time-varying nature of a spin coupled to surrounding spins,

$$\overline{J_{il}(t)J_{il}(t-\tau)} = J_{il}^2 \frac{\overline{\hat{\boldsymbol{S}}_i(\tau)\cdot\hat{\boldsymbol{S}}_i(0)}}{\overline{\hat{\boldsymbol{S}}_i\cdot\hat{\boldsymbol{S}}_i}} \frac{\overline{\hat{\boldsymbol{S}}_l(\tau)\cdot\hat{\boldsymbol{S}}_l(0)}}{\overline{\hat{\boldsymbol{S}}_l\cdot\hat{\boldsymbol{S}}_l}}, \quad (6)$$

with $\hat{\boldsymbol{S}}_i(\tau) = e^{i\tau H_e}\hat{\boldsymbol{S}}_i e^{-i\tau H_e}$. For small τ, since $\hat{\boldsymbol{S}}_i(\tau) \simeq \hat{\boldsymbol{S}}_i + i\tau[H_e, \hat{\boldsymbol{S}}_i] - (\tau^2/2)[H_e, [H_e, \hat{\boldsymbol{S}}_i]]$ [20], $\overline{\hat{\boldsymbol{S}}_i(\tau)\cdot\hat{\boldsymbol{S}}_i(0)} \simeq \overline{\hat{\boldsymbol{S}}_i\cdot\hat{\boldsymbol{S}}_i}e^{-(1/2)\omega_e^2\tau^2}$, where $\omega_e^2 = \sum_l 8J_{il}^2 S(S+1)/3 \simeq 12\bar{J}^2$ and $\bar{J}$ is the average of J_{il}. Hence we obtain $\eta_{il} = \sqrt{\pi}J_{il}^2/\omega_e \simeq \sqrt{\pi/12}J_{il}^2/\bar{J}$.

When $\boldsymbol{M}_i$ is slowly varying in space, the discrete Eq. (4) is reduced to a differential equation,

$$\frac{d\boldsymbol{M}}{dt} = (D_h + D_e)\nabla^2\boldsymbol{M} + \boldsymbol{M}\times\boldsymbol{\omega}, \quad (7)$$

where $D_h = \bar{w}\bar{a}^2$ and $D_e = \bar{\eta}\bar{R}^2 \equiv \sqrt{\pi/12}\bar{J}\bar{R}^2$ are hopping- and exchange-induced spin diffusion (SD) constants. $\bar{w}$ ($\bar{\eta}$) is the ensemble average of w_{ij} (η_{il}), and $\bar{a}$ ($\bar{R}$) is the average intermolecule (interpolaron) distance. In inorganic SI structures, $D_e = 0$, and charge and spin share a common diffusion constant. Another extreme is magnetic insulators, where $D_h = 0$ and spin transport is due exclusively to exchange. For example, in the paramagnetic phase of a Heisenberg model, the SD constant is approximately $|J|R_0^2$, with R_0 being the nearest-neighbor distance between spins [21,22]. We emphasize that the exchange preserves the total spin and does not cause spin relaxation by itself (see Supplemental Material [23]).

The exchange coupling originates from the electron wave function overlap and, for polarons with similar energies, can be estimated by [24,25]

$$\bar{J} = 0.821\frac{e^2}{\epsilon\xi}\left(\frac{\bar{R}}{\xi}\right)^{5/2}\exp(-2\bar{R}/\xi), \quad (8)$$

where ϵ is the dielectric constant, ξ is the polaron localization length, and e is the electron charge. Since $\bar{R}$ is related to the carrier density, $n \equiv \sum_i f_i^0/\mathcal{V}$ with $\mathcal{V}$ being the system volume, via $\bar{R} = n^{-1/3}$, D_e is sensitive to n. Figure 1 plots D_e as well as the ratio $\kappa \equiv D/D_h$ ($D \equiv D_e + D_h$) as a function of n. We set $\epsilon = 2$ and $\xi = 1$ nm, which is the size of a tris-(8-hydroxyquinoline) aluminum (Alq_3) molecule, and fix D_h with its experimental value [16]. It is seen that as n exceeds 10^{17} cm^{-3}, exchange-induced SD becomes significant, and quickly dominates over the hopping-induced SD. For $n > 10^{19}$ cm^{-3}, κ can reach 10^8. Such a carrier density is highly plausible in OSVs. In the recent Hanle experiment [15], a device consisting of 200 nm thick Alq_3 and 2.5 nm thick Al_2O_3 barrier with an area of $A = 1$ mm^2 has a resistance of about 2–20 kΩ. If this resistance comes entirely from the Alq_3 film, according to $R = L/(ne\nu_h A)$ with $\nu_h \simeq 10^{-6}$ cm^2/Vs in Alq_3 at $T = 100$ K, n is estimated at least 10^{18}–10^{19} cm^{-3}. If one takes into account resistance due to the thick Al_2O_3 layer and possible inhomogeneous charge distributions (e.g., filaments), the local carrier density is even higher. It is known that high-density radicals in organics can have a large $\bar{J}$. A good example is diphenyl picryl hydrazyl, whose large exchange $\bar{J}/k_B > 1$ K is responsible for its sharp electron resonance peaks [26].

Now we examine the exchange-induced spin transport under a transverse magnetic field $\boldsymbol{\omega} = \omega\boldsymbol{e}_x$, with the polaron hopping temporarily ignored for simplicity.

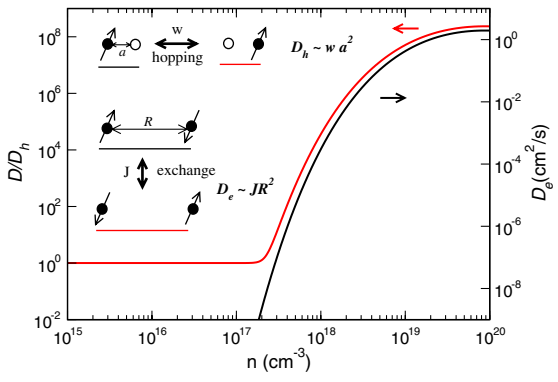

FIG. 1 (color online). SD constant as a function of polaron density. Black and red (gray) lines are D_e and $\kappa = D/D_h$, respectively. $D_h = \nu_h k_B T/e$ with $T = 100$ K and $\nu_h = 10^{-6}$ cm^2/s [16], $\epsilon = 2$, and $\xi = 1$ nm. The inset illustrates hopping- and exchange-induced SD. Solid (open) circles represent occupied (vacant) sites.

We numerically solve Eq. (4) at the steady state ($d\boldsymbol{M}_i/dt = 0$) in a $32 \times 32 \times 32$ cubic lattice with each lattice site representing a polaron. η_{il} is assumed to follow a uniform distribution, $\eta_{il} \in \bar{\eta}[1-\delta, 1+\delta]$. At the two end planes ($x = 0$ and $x = 31\bar{R}$) $\boldsymbol{M}_i$ is fixed at $M_0\boldsymbol{e}_z$. We define $\tau_e \equiv L^2/D = 31^2/\bar{\eta}$ and plot in Fig. 2 $\boldsymbol{M}(x)$, the averaged $\boldsymbol{M}_i$ over the y-z plane for a given x. When $\omega\tau_e \ll 1$, $\boldsymbol{M}(x)$ is uniform across the system. As ω increases, $M_y(x)$ starts to develop and $M_z(x)$ is reduced in the interior of the lattice. When $\omega\tau_e \gg 1$, both $M_y(x)$ and $M_z(x)$ decay rapidly as moving into the interior. The averaged $\overline{M_z}$ over the entire system shows an abrupt decrease around $\omega\tau_e \sim 10$, where the averaged $\overline{M_y}$ reaches the maximum. These features are insensitive to the variance δ in the distribution of η_{il}, and also captured by Eq. (7). The general solution of Eq. (7) is $M_- = M_z - iM_y \sim \exp(\pm e^{i\pi/4}\sqrt{\omega/D}x)$, suggesting an effective SD length of $\sqrt{2D/\omega}$. When this length is smaller than L, M_- diminishes; i.e., the critical magnetic field is $\omega \sim D/L^2 = 1/\tau_e = \kappa D_h/L^2$, which, according to Fig. 1, can be $10^8\times$ larger than D_h/L^2.

When the organic is under a bias, the electric field $\boldsymbol{E}$ causes carrier drift and the charge current is

$$\boldsymbol{j} = en\nu_h\boldsymbol{E} + eD_h\nabla n, \qquad \nu_h = eD_h/k_BT.$$

The electric field also modifies Eq. (4) through w_{ij} but does not affect η_{il} because the exchange-induced spin flip surmounts no energy barrier. The macroscopic spin-current tensor $\overleftrightarrow{j}_S$ can be expressed as

$$j_S^{pq} = j_pM_q + e\nu n\nabla_pB_q + eDn\nabla_pM_q, \tag{9}$$

where the spin drift due to a magnetic-field gradient is included for completeness, $\nu = \mu_BD/k_BT$ (μ_B is the Bohr magneton), and $\nabla_p \equiv \partial/\partial p$. Using the continuity equation of magnetic moment, $(\partial_t + \tau_s^{-1} + \boldsymbol{\omega}\times)n\boldsymbol{M} - \nabla\cdot\overleftrightarrow{j}_S/e = 0$, with τ_s being the spin relaxation time, we obtain the spin transport equation in organics at the steady state,

$$\nabla^2\boldsymbol{M} + \frac{e\boldsymbol{E}}{\kappa k_BT}\cdot\nabla\boldsymbol{M} - \frac{\boldsymbol{M}}{L_s^2} + \boldsymbol{M}\times\frac{\boldsymbol{\omega}}{D} = -\frac{\mu_B}{k_BT}\nabla^2\boldsymbol{B}, \tag{10}$$

where $L_s^2 = D\tau_s$. Compared to the spin-drift-diffusion equation in inorganic semiconductors [27], the spin drift due to an electric field in organics is reduced by a factor of κ and becomes negligible when the carrier density is high.

To directly relate to the Hanle measurements, we study how spin transport and SI depend on ω in the parallel (PA) and antiparallel (AP) configurations of an OSV, an organic film ($0 < x < L$) sandwiched between two ferromagnets (see Fig. 3). Currently a consistent understanding of the MR in OSVs is lacking. However, if the MR arises from SI, it must be due to different spin accumulations at the ferromagnet-organic boundaries. To elucidate the HE, which is controlled by spin transport in the organic bulk, we assume that the two ferromagnets are identical and have no interfacial resistance, although a complete theory of the MR in OSVs likely requires that Schottky barriers [28], spin-dependent interfacial resistances [29], and impurities be included. The spin polarized electrochemical potentials in the ferromagnets satisfy $\nabla^2\Delta\mu - \Delta\mu/L_f^2 = 0$ with $\Delta\mu = \mu_\uparrow - \mu_\downarrow$ and L_f the SD length [30]. The solution at the left ferromagnet ($x < 0$) is

$$\frac{1}{ej}\begin{pmatrix}\mu_\uparrow\\ \mu_\uparrow\end{pmatrix} = \frac{x}{\sigma_\uparrow^L + \sigma_\downarrow^L}\begin{pmatrix}1\\1\end{pmatrix} + c_f\begin{pmatrix}1/\sigma_\uparrow\\ -1/\sigma_\downarrow\end{pmatrix}e^{x/L_f}, \tag{11}$$

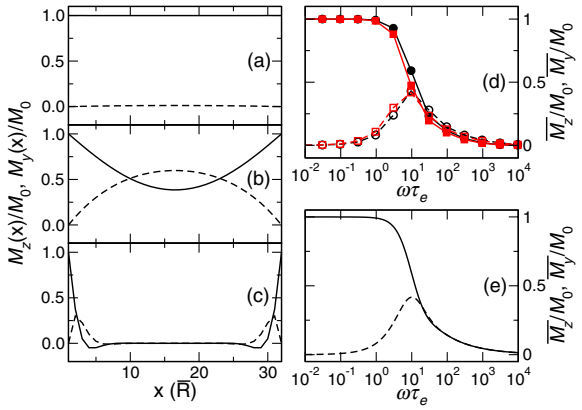

FIG. 2 (color online). Spin polarization in a $32 \times 32 \times 32$ cubic lattice for different transverse magnetic field. Panels (a), (b), and (c) plot spatial distribution of $M_z(x)$ and $M_y(x)$ under $\omega\tau_e = 10^{-1}$, 10, and 10^3. Panels (d) and (e) illustrate the averaged $\overline{M_z}$ and $\overline{M_y}$ as a function ω from solving Eqs. (4) and (7), respectively. Solid and dashed lines are for M_z and M_y. Circles and squares correspond to $\delta = 0$ and 0.6.

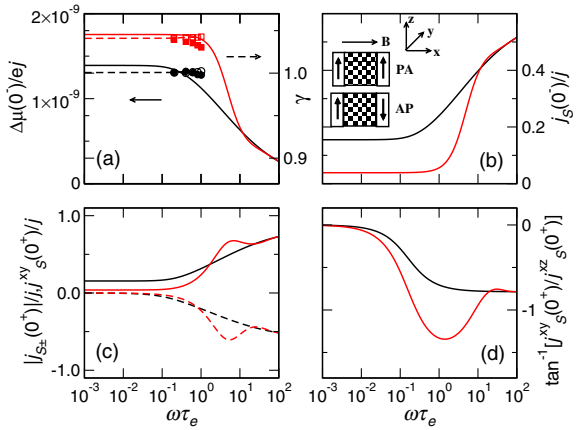

FIG. 3 (color online). Spin accumulation (a), SI efficiency (b), $|J_{S\pm}(0^+)|/j$ (solid line) and $j^{xy}(0^+)/j$ (dashed line) (c), and spin orientation of $\overleftrightarrow{j}_S$ in the organic (d) as a function of ω. Black and gray (red) lines are for the PA and AP configurations. Circles and squares in (a) are γ obtained from Ref. [15] for the PA and AP configurations with squares shifted up by 0.04 in the y axis for clarity. The parameters are $p_f = 0.6$, $L_f = 10$ nm, $T = 100$ K, $n = 6 \times 10^{19}$ cm^{-3}, and $D = 1$ cm^2/V s, $L = 200$ nm, $L_s = 500$ nm.

where $\sigma_{\uparrow(\downarrow)} = [1 + (-)p_f]\sigma_f/2$, with σ_f and p_f being the conductivity and spin polarization of the ferromagnet. The spin-polarized current in the ferromagnet is $ej_{\uparrow(\downarrow)} = \sigma_{\uparrow(\downarrow)}\nabla_x\mu_{\uparrow(\downarrow)}$.

Inside the organic, because of spin precession, the spin-polarized electrochemical potential has both z and y components and can be described by $\mu_\pm = \mu_z \pm i\mu_y$, which is the solution to Eq. (10),

$$\mu_\pm = M_\pm k_B T = a_\pm e^{-\lambda_\pm x} + b_\pm e^{\lambda_\pm (x-L)}, \qquad (12)$$

with $\lambda_\pm = L_s^{-1}(1 \mp i\omega\tau_s)^{1/2}$. Similarly, $\overleftrightarrow{j}_S$ has finite components j_S^{xz} and j_S^{xy} and can be described by $j_{S\pm} \equiv j_S^{xz} \pm ij_S^{xy} = enD\nabla_x M_\pm = (enD/k_BT)\nabla_x\mu_\pm$. Here we focus on the high-κ regime and neglect spin drift due to the electric field in Eqs. (9) and (10). For the PA (AP) configuration, $a_\pm = -(+)b_\pm$. The unknowns $a_\pm$ and c_f can be fixed by the boundary conditions: $\Delta\mu(0^-)$ and $j_S(0^-) \equiv j_\uparrow(0^-) - j_\downarrow(0^-)$ at the ferromagnet are the same as $\mu_\pm(0^+)$ and $j_S^{xz}(0^+)$ at the organic. The obtained spin accumulations for the PA and AP configurations are

$$\left.\frac{\Delta\mu(0^-)}{ej}\right|_{p,a} = p_f\left(G_e g_{p,a}(\theta_+,\theta_-) + \frac{\sigma_f(1-p_f^2)}{2L_f}\right)^{-1}, \qquad (13)$$

where $G_e = e^2nD/(k_BTL)$ is the effective *spin* conductance of the organic, $g_p(\theta_+,\theta_-) = (\theta_+\coth\theta_+ + \theta_-\coth\theta_-)/2$, $g_a(\theta_+,\theta_-) = (\theta_+\tanh\theta_+ + \theta_-\tanh\theta_-)/2$, and $\theta_\pm = \lambda_\pm L/2$. The SI efficiency at the interface is

$$\alpha|_{p,a} \equiv \left.\frac{j_S(0^-)}{j}\right|_{p,a} = \frac{p_f G_e g_{p,a}(\theta_+,\theta_-)}{G_e g_{p,a}(\theta_+,\theta_-) + G_f}. \qquad (14)$$

The spin accumulation causes an additional boundary resistance $R_b = p_f\Delta\mu(0^-)/ej$ [30].

We first inspect the above solutions at $\omega = 0$. We assume $L \ll L_s$ so that carriers retain their spins across the device. For the PA configuration, $g_p(\theta_+,\theta_-) \simeq 1$, the SI efficiency is $\alpha \simeq p_f/(1 + G_f/G_e)$ with $G_f = \sigma_f(1-p_f^2)/(2L_f)$ being the effective conductance of the ferromagnet. If spin transport was due solely to polaron hopping, $D = D_h$, $G_e = G_h \equiv e^2nD_h/(k_BTL)$, where G_h is the *electrical* conductance of the organic, the SI efficiency would be vanishingly small, $\alpha \simeq p_f G_h/G_f \ll 1$, because the low mobility in organics suggests $G_h \ll G_f$. This is the so-called conductivity-mismatch obstacle to SI. However, the effective spin conductance is greatly amplified by the exchange, $G_e = \kappa G_h$, and accordingly, α is enhanced by a factor of κ. Thus the exchange in organic structures effectively circumvents the conductivity-mismatch problem. For the AP configuration, $g_a(\theta_+,\theta_-) = L/L_s \ll 1$, SI is largely blocked. From Eq. (13), the spin accumulation and therefore R_b in the AP configuration are larger than in the PA one, and MR ensues.

Figure 3 shows the spin accumulation and spin current at the ferromagnet-organic interface as a function of ω. For both AP and PA configurations, a finite ω reduces $\Delta\mu(0^-)$ (as well as the device resistance) and increases the SI efficiency α at the interface. Inside the organic, $j_S^{xy}(0^+)$ increases with ω. When $\omega\tau_e \gg 1$, $g_a(\theta_+,\theta_-) = g_p(\theta_+,\theta_-) \simeq \sqrt{2\omega\tau_e}$. Accordingly, $\Delta\mu(0^-)/ej$ (and the MR) diminishes as $\sim 1/\sqrt{\omega\tau_e}$, and α reaches p_f. Inside the organic, $j_S^{xy}(0^+)$ approaches $j_S^{xz}(0^+)$, suggesting that the injected spin is oriented $\pi/4$ away from the electrode's magnetization. Figure 3 also reveals differences between the PA and AP configurations: The HE has a later onset and steeper crossover in the AP configuration ($1 < \omega\tau_e < 10$) than in the PA one ($0.1 < \omega\tau_e < 10$). Moreover, in the AP configuration j_S^{xy} can be much larger than j_S^{xz}, whereas in the PA configuration, j_S^{xy} does not exceed j_S^{xz}. The measured resistance R versus ω in Ref. [15], illustrated as $\gamma \equiv R(\omega)/R(\omega = 0)$ in (a), is consistent with the calculated spin accumulation.

In summary, the exchange between localized carriers in organics can facilitate an efficient spin transport, leading to decoupled spin and charge motions. This spin-charge separation is a key to understanding many puzzles in organic spintronics that seem incompatible with the well-established results on SI, HE, and other spin transport phenomena in inorganic spintronics, and may be exploited for novel organic spintronic devices.

The work was supported by the U.S. Army Research Office under Contract No. W911NF-12-C-0089.

[1] A. Fert, Rev. Mod. Phys. **80**, 1517 (2008).
[2] M. Johnson and R. H. Silsbee, Phys. Rev. B **37**, 5312 (1988).
[3] X. Lou, C. Adelmann, S. A. Crooker, E. S. Garlid, J. Zhang, K. S. M. Reddy, S. D. Flexner, C. J. Palmstrom, and P. A. Crowell, Nat. Phys. **3**, 197 (2007).
[4] N. Tombros, C. Jozsa, M. Popinciuc, H. T. Jonkman, and B. J. van Wees, Nature (London) **448**, 571 (2007).
[5] I. Appelbaum, B. Huang, and D. J. Monsma, Nature (London) **447**, 295 (2007).
[6] D. H. Hernando, Yu. V. Nazarov, A. Brataas, and G. E. W. Bauer, Phys. Rev. B **62**, 5700 (2000).
[7] Nat. Mater. **8**, 691 (2009).
[8] V. Dediu, M. Murgia, F. C. Matacotta, C. Taliani, and S. Barbanera, Solid State Commun. **122**, 181 (2002).
[9] Z. H. Xiong, D. Wu, Z. V. Vardeny, and J. Shi, Nature (London) **427**, 821 (2004).
[10] V. Dediu, L. E. Hueso, I. Bergenti, A. Riminucci, F. Borgatti, P. Graziosi, C. Newby, F. Casoli, M. P. De Jong, C. Taliani, and Y. Zhan, Phys. Rev. B **78**, 115203 (2008).
[11] A. J. Drew, J. Hoppler, L. Schulz, F. L. Pratt, P. Desai, P. Shakya, T. Kreouzis, W. P. Gillin, A. Suter, N. A. Morley, V. K. Malik, A. Dubroka, K. W. Kim, H. Bouyanfif, F. Bourqui, C. Bernhard, R. Scheuermann, G. J. Nieuwenhuys, T. Prokscha, and E. Morenzoni, Nat. Mater. **8**, 109 (2009).

[12] D. L. Sun, L. Yin, C. Sun, H. Guo, Z. Gai, X.-G. Zhang, T. Z. Ward, Z. Cheng, and J. Shen, Phys. Rev. Lett. **104**, 236602 (2010).
[13] X. Zhang, S. Mizukami, T. Kubota, Q. Ma, M. Oogane, H. Naganuma, Y. Ando, and T. Miyazaki, Nat. Commun. **4**, 1392 (2013).
[14] M. Grünewald, M. Wahler, P. Grazioso, A. Dediu, F. Würthner, G. Schmidt, and L. W. Molenkamp, in *Proceedings of SPINOS, 2010* (unpublished).
[15] A. Riminucci, M. Prezioso, C. Pernechele, P. Graziosi, I. Bergenti, R. Cecchini, M. Calbucci, M. Solzi, V. A. Dediu, Appl. Phys. Lett. **102**, 092407 (2013).
[16] See, e.g., H. Mu, D. Klotzkin, A. de Silva, H. P. Wagner, D. White, and B. Sharpton, J. Phys. D **41**, 235109 (2008).
[17] G. Schmidt, D. Ferrand, L. W. Molenkamp, A. T. Filip, and B. J. van Wees, Phys. Rev. B **62**, R4 790 (2000).
[18] We neglect the indirect exchange caused by the second-order process of H_h when adjacent molecules are both occupied by polarons, which requires $n \sim 10^{21}$ cm^{-3}.
[19] C. P. Slichter, *Principles of Magnetic Resonance* (Springer-Verlag, Berlin, 1978), 2nd ed.
[20] Cumulant expansion yields $\overline{\hat{\boldsymbol{S}}_i(\tau)\cdot\hat{\boldsymbol{S}}_i} = \hat{\boldsymbol{S}}_i\cdot\hat{\boldsymbol{S}}_i\cosh^{-2}(\omega_e t/2\sqrt{2})$ and $\eta_{il} = 8\sqrt{2}J_{il}^2/3\omega_e$.
[21] P. G. de Gennes, J. Phys. Chem. Solids **4**, 223 (1958).
[22] H. S. Bennett and P. C. Martin, Phys. Rev. **138**, A608 (1965).
[23] Supplemental Material at http://link.aps.org/supplemental/10.1103/PhysRevLett.111.016601 for the exchange effects on spin relaxation and diffusion.
[24] C. Herring and M. Flicker, Phys. Rev. **134**, A362 (1964).
[25] M. I. Chibisov and R. K. Janev, Phys. Rep. **166**, 1 (1988).
[26] J. P. Goldsborough, M. Mandel, and G. E. Pake, Phys. Rev. Lett. **4**, 13 (1960).
[27] Z. G. Yu and M. E. Flatté, Phys. Rev. B **66**, 201202(R) (2002); **66**, 235302 (2002).
[28] P. P. Ruden and D. L. Smith, J. Appl. Phys. **95**, 4898 (2004).
[29] E. I. Rashba, Phys. Rev. B **62**, R16267 (2000).
[30] P. C. van Son, H. van Kempen, and P. Wyder, Phys. Rev. Lett. **58**, 2271 (1987).